Modeling of Asymmetric Membrane Formation. II. The Effects of Surface Boundary Conditions

L. YILMAZ and A. J. McHUGH* *Department of Chemical Engineering, University of Illinois, Urbana, Illinois 61801*

Synopsis

An analysis is carried out to evaluate the effects of alternate surface boundary conditions on the predictions of our previously developed (Part I) pseudobinary diffusion model for membrane formation by the phase inversion process. Attention is addressed to a comparison of concentration profiles in the quenched film for a constant flux interface (CF) condition and a mass transfer rate (MT) interface condition. A numerical algorithm is developed to handle the MT condition based on an explicit, finite difference marching method. Comparison of concentration profiles with those obtained earlier for the CF boundary condition show that since results for both cases are very similar, either condition can be used in concentration profile calculations. Changes in bath conditions will mainly affect membrane formation through the changed solvent/nonsolvent flux ratio during quenching.

INTRODUCTION

The field of membrane science and technology has undergone an enormous growth since the discovery that asymmetric skinned structures can be formed by the so-called phase-inversion process involving casting a solution of a polymer in a solvent (or mixture of solvents) followed by quenching in a nonsolvent bath.[1] The widespread application of such membranes has generated numerous studies on the conditions and possible mechanisms for the formation of the characteristic morphologies during and after phase inversion.[2-8] Despite this high level of activity, however, relatively few attempts have been made to quantify and/or systematize the information in terms of models for the structure formation. Therefore, in a recent paper[9] (to be referred to as Part I) we presented a systematic modeling approach emphasizing both the thermodynamic and kinetic aspects of phase inversion during the quench period. A pseudobinary diffusion formalism was developed and used in conjunction with an analysis of the ternary phase diagram behavior of typical membrane forming systems[10] to evaluate the phase separation characteristics. The advantages, predictive power, and potential for further use of this approach were also discussed in detail.

An important feature of the pseudobinary formalism is that the mixing rule decouples from the diffusion equations, thus allowing one to easily superpose composition paths on the ternary phase diagram and study these independently of the concentration development as a function of time and distance in

*Author to whom correspondence should be addressed.

Journal of Applied Polymer Science, Vol. 35, 1967–1979 (1988)

CCC 0021-8995/88/071967-13$04.00

the film. As discussed in Part I, however, choice of the appropriate surface boundary condition for the latter calculation is one of the more complicated and controversial issues of the mass transfer modeling.[11-14] In this paper this aspect of the problem is discussed in more detail by assessing both the nature and degree of effect of alternate boundary conditions on the computed concentration profiles. In such a fashion one can also gain some feel for the importance of specific recipe conditions on the membrane formation characteristics. Likewise, since changes in the bath conditions (i.e., by stirring or introducing convective current effects) can affect both the surface boundary condition and the solvent–nonsolvent flux ratio k', a knowledge of one (e.g., BC effects) should enable determining the probable role of the other, thereby improving the predictive capacity of the pseudobinary model. Since control of the bath-side conditions is relatively easy, such information should also aid in the design of desired membrane structures.

We begin with a brief discussion of the pseudobinary model and the associated alternate surface boundary conditions, followed by a detailed analysis of the concentration profiles.

PSEUDOBINARY DIFFUSION EQUATIONS

The pseudobinary diffusion model starts from the assumption that, due to the highly entangled nature of the casting solution, the polymer mass flux $\mathbf{n}_3$ will be negligible compared to that of the nonsolvent, $\mathbf{n}_1$, or solvent, $\mathbf{n}_2$. Thus by defining liquid density ρ and mass fractions ω_i on a polymer-free basis, the nonsolvent flux equation becomes

$$\mathbf{n}_1 = -\bar{\rho}D\nabla\bar{\omega}_1 + \bar{\omega}_1(\mathbf{n}_1 + \mathbf{n}_2) \tag{1}$$

In this expression, D is a concentration-dependent phenomenological diffusion coefficient and overbars are used to signify a polymer-free basis. Combination with the equations of continuity

$$\frac{\partial\bar{\rho}}{\partial t} = -\nabla\cdot(\mathbf{n}_1 + \mathbf{n}_2) \tag{2}$$

$$\frac{\partial\bar{\rho}_1}{\partial t} = -\nabla\cdot\mathbf{n}_1 \tag{3}$$

leads to the following equations for diffusion in the z direction (measured into the film relative to the bath interface position, $z = 0$):

$$\bar{\rho}\frac{\partial\bar{\omega}_1}{\partial t} = \frac{\partial}{\partial z}\left(D\bar{\rho}\frac{\partial\bar{\omega}_1}{\partial z}\right) - \frac{k\bar{\rho}D}{(1 + k\bar{\omega}_1)}\left(\frac{\partial\bar{\omega}_1}{\partial z}\right)^2 \tag{4}$$

$$\frac{\partial\bar{\rho}}{\partial t} = -\frac{\partial}{\partial z}\left(\frac{k\bar{\rho}D}{1 + k\bar{\omega}_1}\frac{\partial\bar{\omega}_1}{\partial z}\right) \tag{5}$$

where $k = k' - 1$ and $k' = -\mathbf{n}_2/\mathbf{n}_1$. Since experimental observations[2-5] have shown that the skin forms very quickly as a thin layer at the surface, our

calculations are necessarily restricted to short times and distances from the interface. Thus, taking k to be independent of position, the previous set of equations reduces to

$$\frac{\partial \bar{\rho}}{\partial \bar{\omega}_1} = \frac{-k\bar{\rho}}{(1 + k\bar{\omega}_1)} \tag{6}$$

As mentioned, the question of appropriate initial and, most especially, boundary conditions needed to obtain a well-posed set of equations is to some extent a controversial aspect of the modeling. In the absence of an evaporation step, the first four of these would be straightforward and can be written as follows:

$$\bar{\rho} = \bar{\rho}_i \qquad \text{at } t = 0,\ z > 0 \text{ and as } z \to \infty \text{ for all } t > 0 \tag{7}$$

$$\bar{\omega}_1 = \bar{\omega}_{1i} \qquad \text{at } t = 0,\ z > 0 \text{ and as } z \to \infty \text{ for all } t > 0 \tag{8}$$

where subscripts i refer to constant initial values. In most cases the initial nonsolvent composition would in fact be zero, i.e., $\bar{\omega}_{1i} = 0$. The question of alternate boundary conditions at the bath–film interface is considered in the next section.

SURFACE BOUNDARY CONDITIONS

The quench period mass transfer model developed by Cohen et al.[11] neglected mass transfer in the bath by assuming that the surface of the film instantaneously equilibrates with the bulk composition of the bath. Thus surface concentrations were taken as constant during the quench process. For a number of reasons this is a very problematic assumption. First of all, there are experimental observations that contradict this assumption. For some cases Cabasso[15] observed accumulation of a solvent layer in the bath next to the film surface, and in other cases he observed a convective flow of solvent emanating from the polymer film. Both of these observations imply bath side mass transfer. In addition, a number of studies[6,15,16] have indicated that mass transfer on the bath side of the interface can have a strong influence on the structure of the formed membrane. For example, asymmetric structures can result when a nonsolvent liquid is used in the quench bath while, if the film is quenched in a nonsolvent vapor environment, the result is a completely porous membrane.[16,17] Elimination of this assumption then leaves two equally plausible choices, either of which can be justified qualitatively on the basis of experimental observations for different membrane forming systems. The first choice (used exclusively in Part I) is that of constant flux at the surface and is based on the above-mentioned study,[15] indicating that, for many systems, a fast, convective flow of solvent occurs into the bath resulting from the density difference between the solvent and nonsolvent. Thus the constant flux condition (CF) can be written as

$$\mathbf{n}_1|_{z=0} = \text{const} \tag{9a}$$

and

$$\mathbf{n}_2|_{z=0} = \text{const} \tag{9b}$$

These relations thus imply that $k'|_{z=0}$ will be constant, and, since, by assumption, $k'(z) = k'|_{z=0}$, one has that the flux ratio will be constant throughout the diffusion path. Hence eq. (6) can be integrated, subject to eqs. (7) and (8), to yield the following important relation between the liquid density and k

$$\bar{\rho} = \frac{(1 + k\bar{\omega}_{1i})\bar{\rho}_i}{1 + k\bar{\omega}_1} \tag{10}$$

We note that eq. (10), which has been obtained without having to solve eqs. (4) and (5), directly serves as the basis for construction of composition paths on the ternary phase diagram as given in Part I.

The second and equally plausible surface condition is based on qualitative experimental observations reported by Strathmann and co-workers,[16,18] suggesting the existence of a mass transfer boundary layer on the bath side. This condition (referred to as MT) can be formulated as follows:

$$\mathbf{n}_1|_{z=0} = \rho_{\text{bath}} k_1 (\omega_{1b} - \bar{\omega}_1|_{z=0}) \qquad \text{at } z = 0 \text{ and } t > 0 \tag{11a}$$

$$\mathbf{n}_2|_{z=0} = \rho_{\text{bath}} k_2 (\omega_{2b} - \bar{\omega}_2|_{z=0}) \qquad \text{at } z = 0 \text{ and } t > 0 \tag{11b}$$

where ρ_{bath} is the bath side liquid density, subscript b refers to bath side conditions, and the k_i are mass transfer coefficients. Using the fact that $\bar{\omega}_1 + \bar{\omega}_2 = 1$ leads to the following

$$\frac{-\mathbf{n}_2|_{z=0}}{\mathbf{n}_1|_{z=0}} = \frac{k_2}{k_1} = k'|_{z=0} = \text{const} \tag{12}$$

Hence one finds that the flux ratio will be constant for this case as well and the relation between liquid density and flux ratio, i.e., eq. (10), remains unchanged as do the predictions and conclusions based on the superposed ternary profiles.[9] Thus the differences between the two boundary conditions will be shown in the various component profiles as a function of time and position in the film. To assess this effect, one needs to solve the defining diffusion equation.

CONCENTRATION PROFILES FOR MT BOUNDARY CONDITION

Since the flux ratio k remains constant, eq. (10) can be substituted in eq. (4) to yield the following diffusion equation for constant $D = D_0$:

$$\frac{1}{1 + k\bar{\omega}_1} \frac{\partial \bar{\omega}_1}{\partial t} = D_0 \frac{\partial}{\partial z} \left(\frac{1}{1 + k\bar{\omega}_1} \frac{\partial \bar{\omega}_1}{\partial z} \right) - \frac{kD_0}{(1 + k\bar{\omega}_1)^2} \left(\frac{\partial \bar{\omega}_1}{\partial z} \right)^2 \tag{13}$$

Combination of eqs. (1), (10), and (11a) gives the following expression for the

surface boundary condition:

$$\frac{\rho_{\text{bath}}}{\bar{\rho}_i^*} k_1(\omega_{1b} - \bar{\omega}_1|_{z=0}) = -\left(\frac{D_0}{(1 + k\bar{\omega}_1)^2} \frac{\partial \bar{\omega}_1}{\partial z} \right)\Bigg|_{z=0}, \qquad \text{for } t > 0 \quad (14)$$

where $\bar{\rho}_i^* = (1 + k\bar{\omega}_{1i})\bar{\rho}_i$. Together with eqs. (7) and (8), one then has a properly posed equation set to solve for the nonsolvent concentrations as a function of time and position. Introducing the transformation variable $f = k\bar{\omega}_1/(1 + k\bar{\omega}_1) - k\bar{\omega}_{1i}/(1 + k\bar{\omega}_{1i})$, a dimensionless time, $\tau = (k_1\omega_{1b})^2 t/D_0$ and a dimensionless distance $x = z/L_0$ with L_0 being the initial film thickness, leads to the following equation set to be solved:

$$\frac{\partial f}{\partial \tau} = \alpha^2 \frac{\partial^2 f}{\partial x^2} \quad (15)$$

$$f(x,0) = 0 \quad (16)$$

$$f(\infty, t) = 0 \quad (17)$$

$$-a_1 + \frac{a_1}{k\omega_{1b}} \left(\frac{f}{1-f} \right)\Bigg|_{x=0} = \frac{\partial f}{\partial x}\Bigg|_{x=0} \quad (18)$$

where

$$a_1 = \frac{k\rho_{bath}}{\bar{\rho}_i^* \alpha} \qquad \text{and} \qquad \alpha = \frac{D_0/L_0}{k_1\omega_{1b}}$$

Although the mathematical definition of α differs here from that used for the constant flux condition in Part I, we note that its physical significance as a ratio of external to internal mass transfer resistances remains the same. Introduction of the MT condition produces an important mathematical consequence, however, in that since eq. (18) is nonlinear, analytical solution is no longer possible,[19,20] necessitating use of a numerical integration scheme.

SOLUTION SCHEME

To handle the semi-infinite boundary condition, an explicit finite difference marching method has been selected. Use of an implicit (or semi-implicit) method would require assigning an arbitrary condition for infinity, and this position would have to be changed with progression in time. Likewise, the selection of such a condition needs to be checked by repeated calculation of concentration profiles at the same time value for different positions assumed as infinity, which makes the treatment more difficult. Since an explicit method is used, the $+x$ direction can be left open.[21] Calculation of the concentration profile at time t is simply terminated when $f(x, t)$ becomes smaller than a preselected fixed value ϵ without the need to know x, which is a function of time, beforehand.

It was decided to employ a variable grid in which increments in space, Δx, depend on both time and position. The reason for choosing a time-dependent discretization is that, due to the developing concentration field with time, Δx can be increased at large times without jeopardizing the numerical accuracy.

Since concentration gradients will be much steeper near the film–bath interface, more grid points are necessary in that region. Thus Δx is also made position-dependent. Finite difference forms for the differential equation are given by the following:

$$f_{j,n+1} = f_{j,n} + r_1(f_{j+1,n} - 2f_{j,n} + f_{j-1,n}) \qquad \text{for } 0 < j < J \tag{19}$$

$$f_{j,n+1} = f_{j,n} + r_2(f_{j+1,n} - (1 + p_1)f_{j,n} + p_1 f_{j-1,n}) \qquad \text{for } j = J \tag{20}$$

$$f_{j,n+1} = f_{j,n} + \frac{r_1}{p_1^2}(f_{j+1,n} - 2f_{j,n} + f_{j-1,n}) \qquad \text{for } J < j \leq j_1 \tag{21}$$

$$f_{j_1,n+1} \leq \epsilon \tag{22}$$

where

$$r_1 = \alpha^2 \frac{\Delta\tau}{(\Delta x)_n} \qquad \text{and} \qquad r_2 = r_1 \frac{2}{p_1(1 + p_1)}$$

When the total grid point number for a specific time τ (i.e., j_1) exceeds a preset limit M, the space increment is automatically increased as $(\Delta x)_{n+1} = p_2(\Delta x)$.

The surface condition is treated by introducing a fictitious grid point,[22] and therefore surface concentration can be expressed (after manipulations) as

$$f_{0,n+1} = f_{0,n} + 2r_1(f_{1,n}) + (\Delta x)_n a_1 - f_{0,n}\left(1 + \frac{\Delta x a_1}{k\omega_{1b}} \frac{1}{1 - f_{0,n}}\right)$$

$$\text{for } j = 0 \tag{23}$$

Thus the complete finite difference description of the system is given by eqs. (19)–(23).

For stability reasons r_1 needs to be smaller than 0.5, which in combination with the uniform initial condition leads to the realization that, regardless of how small the selected time increment is, for the first time step calculation (i.e., $n = 1$), the number of grid points available for computation will be very small. Thus an asymptotic solution valid for very small times was used as an initial condition and the numerical solution algorithm was initiated at $\tau = \Delta\tau$ instead of at $\tau = 0$. To do this, a Taylor series expansion was first applied to the surface boundary condition retaining only the first term for small f values. The boundary condition can thus be expressed as

$$-a_1 + \frac{a_1}{k\omega_{1b}} f\Big|_{x=0} = \frac{\partial f}{\partial x}\Big|_{x=0} \tag{24}$$

Since this is a linear condition, eq. (15) can be solved analytically, resulting in the following:

$$f = k\omega_{1b}\left(\operatorname{erfc}\left(\frac{x}{\sqrt{4\alpha^2\tau}}\right) - \exp(hx + h^2\alpha^2\tau) \quad \operatorname{erfc}\left(\frac{x}{\sqrt{4\alpha^2\tau}} + h\sqrt{\alpha^2\tau}\right)\right) \tag{25}$$

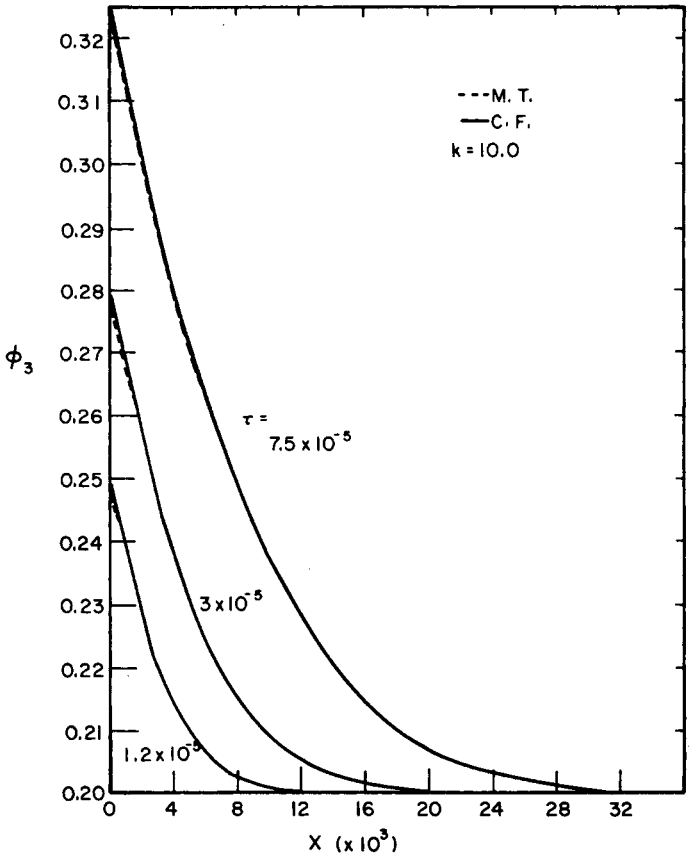

Fig. 1. Polymer volume fraction profiles in the quenched film for two different boundary condition cases at different dimensionless times: (---) MT; (——) CF; k = 10.0.

where

$$h = \frac{a_1}{k\omega_{1b}}$$

The above expression, evaluated at $\tau = \Delta\tau$, was then used to start up the numerical solution. The numerical algorithm and selections for values of the numerical parameters were first tested by using the constant flux boundary condition for which the complete analytical solution is known (given in Part I). Comparison of analytical and numerical results demonstrated the accuracy of our numerical method.

RESULTS AND DISCUSSION

To investigate effects of the surface boundary condition on concentration profiles, results obtained using CF boundary condition and MT boundary condition are plotted together in Figures 1–6.

The principal conclusion derived from such plots (as well as from the overall calculations) is that concentration profiles for CF and MT surface boundary

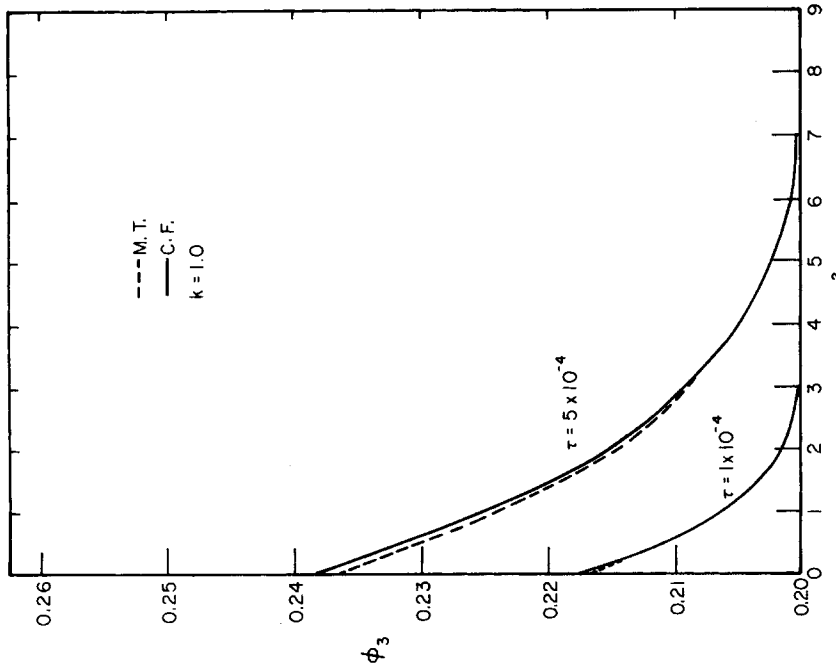

Fig. 2. Polymer volume fraction profiles in the quenched film for two different boundary condition cases at different dimensionless times: (---) MT; (——) CF; $k = 1.0$.

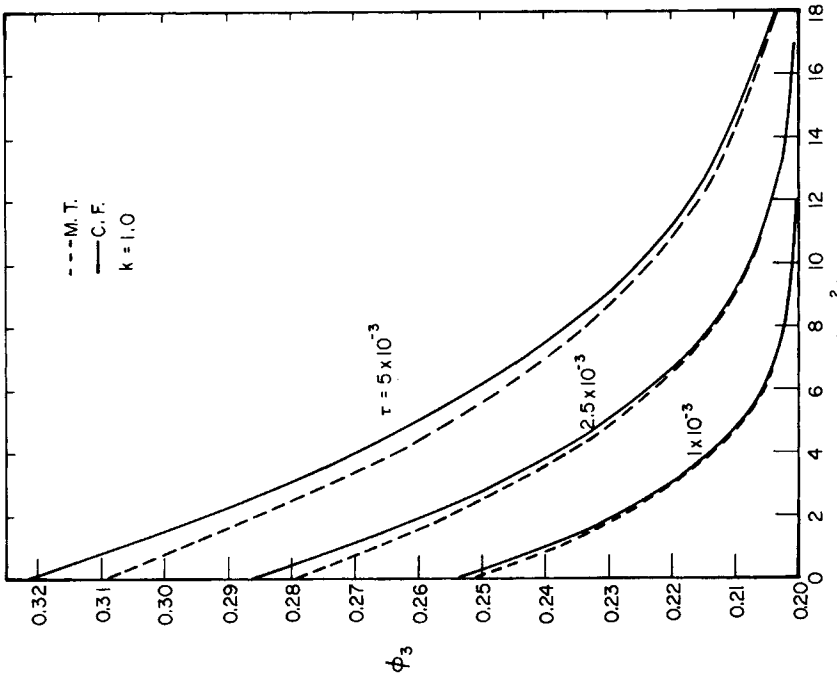

Fig. 3. Polymer volume fraction profiles in the quenched film for two different boundary condition cases at different dimensionless times: (---) MT; (——) CF; $k = 1.0$.

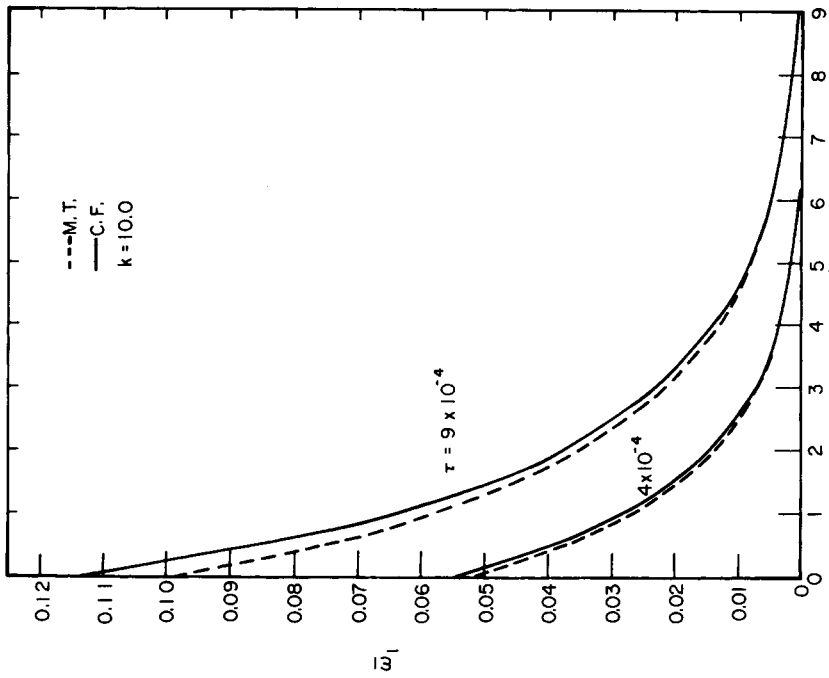

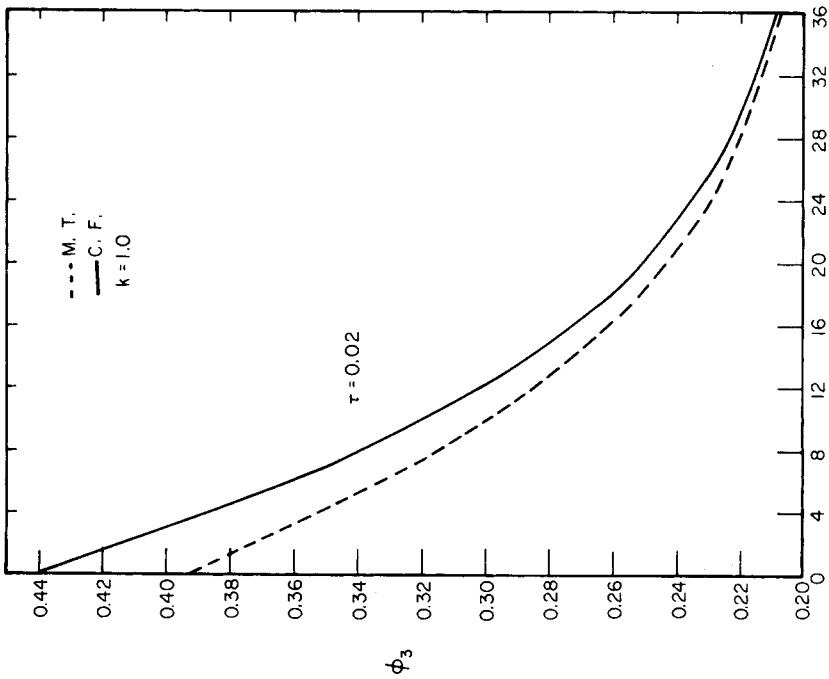

Fig 4. Polymer volume fraction profiles in the quenched film for two different boundary condition cases at a large dimensionless time value: (---) MT; (——) CF; $k = 1.0$.

Fig. 5. Nonsolvent weight fraction (polymer-free) profile in the quenched film for two different boundary condition cases at different dimensionless times: (---) MT; (——) CF; $k = 10.0$.

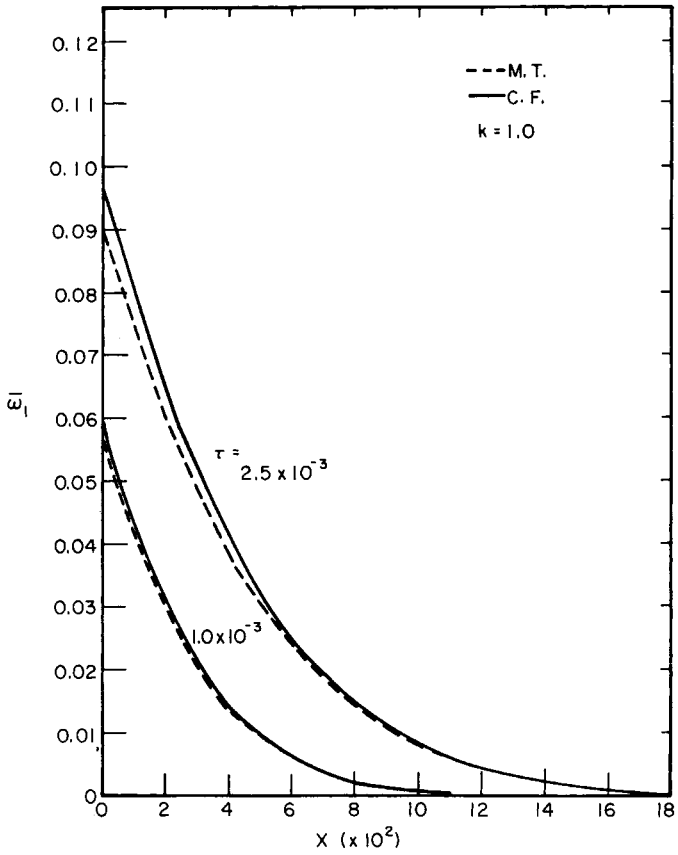

Fig. 6. Nonsolvent weight fraction (polymer-free) profile in the quenched film for two different boundary condition cases at different dimensionless times: (---) MT; (——) CF; $k = 1.0$.

condition cases are very similar over a wide range of system parameter values (i.e., k, α, ϕ_{3i}, ρ_2^0, etc.). Figures 1–3 show that, for small times, profiles are essentially identical and in the medium time range differences are small. As mentioned previously, the relevant range for our problem is that of short times and distances (restrictions in fact used in the construction of our mathematical formalism). Thus concentration profiles at small times (especially portions of profiles that are next to the surface) are the meaningful ones for our discussion. Examination of the relevant figures, emphasizing these curves and curve parts, clearly shows the close agreement resulting from the two different boundary condition cases. To see any important difference between these two cases, concentration profiles at large times, as exemplified in Figure 4, have to be considered; however, this is not relevant to our discussion.

Examination of Figures 3 and 5 shows that even when the MT solution begins to deviate from that for CF, the general shapes and characteristics of the profiles still remain similar. This is an important observation since it places the predictions concerning general membrane morphology and skin structure, made in Part I, on a more solid footing independent of the selection

of the surface boundary condition but a general characteristic of our model and of general membrane forming system.

For the situations where MT results deviate from CF results, the entire curves move to lower concentration levels, as demonstrated by Figures 3 to 5. This is a rather surprising observation since it is expected that effects of different surface boundary conditions would propagate from the surface. However, we feel that this observation strengthens the arguments of the preceding paragraph in that since the entire curves shift while still maintaining the same general features (slopes, etc.) (and since we are more interested in the qualitative characteristics rather than exact values of dimensionless time and distance), then the surface boundary conditions will not significantly affect any predictions for membrane formation. At large times surface slopes for MT cases become smaller than those for CF cases.

To see whether or not using a different surface boundary condition affects different concentration profiles to a different degree, an investigation of the relative effects of surface boundary conditions on $\bar{\omega}_1$ and ϕ_3 was made. Comparison of Figures 3 and 6 and examination of Figure 5 demonstrates that such effects are similar, both qualitatively and quantitatively.

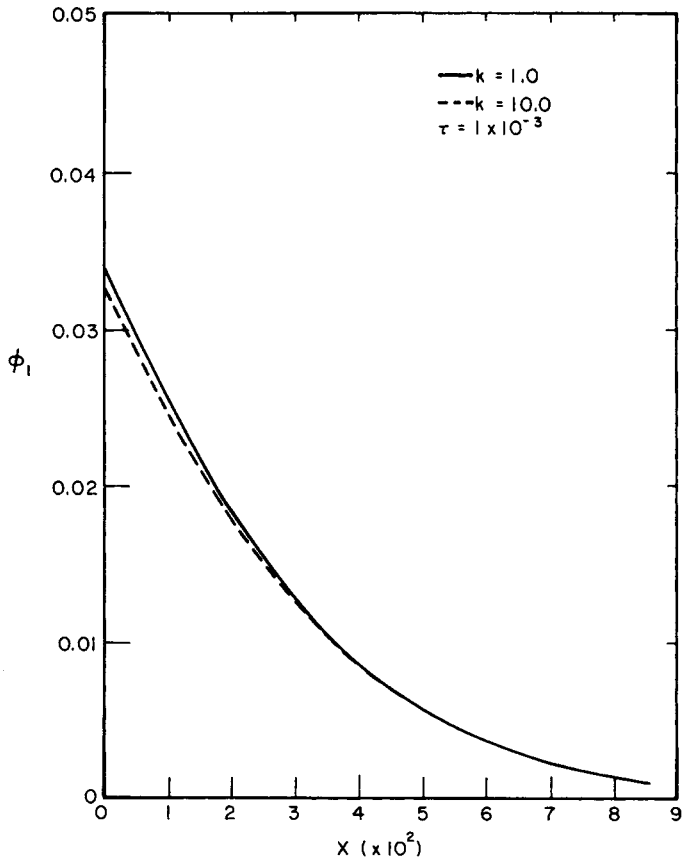

Fig. 7. Nonsolvent volume fraction profiles in the quenched film for the MT case for various flux ratios: (——) $k = 1.0$; (---) $k = 10.0$; $\tau = 1 \times 10^{-3}$.

Examination of Figures 2 and 5 shows that differences between the concentration profiles decrease with increasing flux ratio k. Thus one concludes that, for the high flux ratio range, concentration profile characteristics will be dominated mainly by the flux ratio.

Up to this point, only polymer volume fraction profiles and nonsolvent mass fraction (on a polymer-free basis) profiles have been discussed. Examination of nonsolvent volume fraction profiles is also necessary and will be useful for structure predictions and for further studies at step c (Part I) of our systematization. The analytical expression for the nonsolvent fraction profile for the CF case (given in the Part I) shows that it is independent of flux ratio. Figure 7 shows that, for the MT case, although the ϕ_1 profile does depend on the value of the flux ratio, the effect is extremely small. Also, from this figure, it can be observed that general shapes and features of the ϕ_1 profiles are similar to those of the ϕ_3 profiles.

CONCLUSIONS

Based on the preceding discussion, some general useful conclusions can be reached concerning the effects and selections of surface boundary conditions. First of all it can be concluded that both the constant flux interface and mass transfer surface boundary condition expressions could be used in concentration profile calculations and therefore for structure predictions. Therefore, there is no need to attempt to determine which one of those is operational for a specific system; selection of boundary condition could be merely based on mathematical convenience.

Secondly, based on these calculations, we can conclude that any change made in conditions of the bath will affect membrane formation mainly through changing flux ratio values. This finding could be useful in prediction and even in design of new membrane structures.

References

1. S. Loeb and S. Sourirajan, U.S. Pat. 3,133,132 (1964).
2. H. K. Lonsdale and H. E. Podall (Eds.), *Reverse Osmosis Membrane Research*, Plenum, New York, 1972.
3. S. Sourirajan (Ed.), *Reverse Osmosis and Synthetic Membranes*, National Research Council of Canada, Ottawa, 1977.
4. V. T. Stannet, W. J. Koros, D. R. Paul, H. K. Lonsdale, and R. W. Baker, *Adv. Polym. Sci.*, **32**, 69 (1979).
5. L. Dresner and J. S. Johnson, in *Principles of Desalination*, K. S. Spiegler and A. D. K. Laird, Eds., Academic, New York, 1980.
6. R. E. Kesting, *Synthetic Polymeric Membranes*, Wiley, New York, 1985.
7. D. R. Lloyd, (Ed.), *Materials Science of Synthetic Membranes*, ACS Symp. Ser. 269, American Chemical Society, Washington, DC, 1985.
8. E. Drioli and M. Nakagaki (Eds.), *Membranes and Membrane Processes*, Plenum, New York, 1986.
9. L. Yilmaz and A. J. McHugh, *J. Memb. Sci.*, **28**, 287 (1986).
10. L. Yilmaz and A. J. McHugh, *J. Appl. Polym. Sci.*, **31**, 997 (1986).
11. C. Cohen, G. B. Tanny, and S. Prager, *J. Polym. Sci., Polym. Phys. Ed.*, **17**, 477 (1979).
12. R. J. Ray, Ph.D. thesis, University of Colorado, 1983.
13. J. G. Wijmans, F. W. Altena, and C. A. Smolders, *J. Polym. Sci., Polym. Phys. Ed.*, **22**, 519 (1984).
14. A. J. McHugh and L. Yilmaz, *J. Polym. Sci., Polym. Phys. Ed.*, **23**, 127 (1985).

15. I. Cabasso, in *Synthetic Membranes*, A. F. Turbak, Ed., ACS Symp. Ser. 153, American Chemical Society, Washington, DC, 1981.
16. H. Strathmann and K. Kock, *Desalination*, **21**, 241 (1977).
17. H. Strathmann, P. Scheible, and R. W. Baker, *J. Appl. Polym. Sci.*, **15**, 811 (1971),
18. H. Strathmann, K. Kock, and P. Amar, *Desalination*, **21**, 241 (1977).
19. J. Crank, *The Mathematics of Diffusion*, Clarendon, Oxford, 1975.
20. L. Dresner, *Similarity Solutions of Partial Differential Equations*, Pitman, Boston, 1983.
21. D. K. An, *Phys. Stat. Sol.* (*a*), **90**, 1973 (1985).
22. G. D. Smith, *Numerical Solution of Partial Differential Equations*, Clarendon, Oxford, 1978.

Received September 15, 1987
Accepted September 21, 1987